

# Influence of boundaries on the imaging of objects in turbid media

J. C. J. Paasschens

*Philips Research Laboratories, Prof. Holstlaan 4, 5656 AA Eindhoven, The Netherlands, and Instituut-Lorentz, University of Leiden, P.O. Box 9506, 2300 RA Leiden, The Netherlands*

G. W. 't Hooft

*Philips Research Laboratories, Prof. Holstlaan 4, 5656 AA Eindhoven, The Netherlands*

Received September 24, 1997; revised manuscript received January 15, 1998; accepted February 10, 1998

To image objects that are present in a random medium, one needs to know how sensitive measurements are to different kinds of objects and to the position of those objects. Within the diffusion theory we generalize expressions that describe the sensitivity to extra scattering and extra absorption. The sensitivity is influenced by the geometry and by the boundaries of the medium. We describe how sources and detectors at different boundaries have to be handled theoretically. We then compare an unbounded medium, a medium having a black boundary, and a medium having a mirror as a boundary and study the differences in sensitivity. Our results are confirmed by experiments. © 1998 Optical Society of America [S0740-3232(98)00307-X]

*OCIS codes:* 000.6800, 100.6950, 110.4850, 120.5820, 170.3660, 290.1990.

## 1. INTRODUCTION

For imaging the interior of a turbid medium, several methods have been developed in the recent past. The imaging consists of two parts. First, one has to define a geometry and a measurement. Next, one has to reconstruct the interior of the medium with the data. For detection one has at one's disposal, apart from continuous-wave measurements, the time-resolved measurements and the photon-density-wave approach. For reconstruction one uses, among others, backprojection and algebraic reconstruction techniques. Both detection and reconstruction depend on the geometry of the medium, the positions of sources and detectors, and the character of the objects that one wants to image.

Two factors are of experimental importance in detecting the object. The first is the accuracy of the measurements. In practice, this depends on the strength of the signal: the larger the signal, the less the relative noise and therefore the larger the accuracy. The second is the sensitivity to inhomogeneities. This depends on the measurement method as well as on the position of the object with respect to the source and the detector. For a given accuracy one can ask the question, what kind of objects can still be detected and possibly reconstructed? Which measurement method is the best? Furthermore, since the boundaries are of influence on the measured signal, one can ask, which kind of boundary is best for imaging?

To address these questions, we will start with the calculation of the influence of an object on the measured signal. We are mainly interested in the order of magnitude of the effect, so that we can give a reasonable estimate of the accuracy needed to detect an object. We will generalize the methods given by den Outer *et al.*<sup>1</sup> and Zhu *et al.*<sup>2</sup> to be able to split the effect of an object on a measurement into a geometry-dependent part—including

boundaries, sources, and detectors—and a pure-object-dependent part. Both parts depend furthermore on the optical parameters of the medium and possibly on the frequency of the amplitude modulation of the source. Time-dependent sources are related to the latter by a Fourier transform.

The treatment will lead to general formulas to estimate the effect of objects on measurements for general geometries. We can then include the influence of the boundaries of the medium and compare these with measurements in an infinite medium. We will basically consider two kinds of boundaries. The first are those that reflect the major part of the light. This reflection can be due, for instance, to a mirror. The second boundary to be considered is that consisting of a transparent medium surrounding the turbid medium, with possible refractive-index mismatch. When this mismatch vanishes, none of the light leaving the turbid medium will be reflected back and the boundary is equivalent to a completely black boundary.

To discuss the effects of boundaries, we will consider the two basic classes of measurements, those in reflection and those in transmission. In the first case we will consider a semi-infinite medium; in the second, a slab geometry. In both cases the source and the detector are located at the surface. We argue that our results are qualitatively the same for other, possibly more complex geometries.

The outline of this study is as follows. In Section 2 we will calculate the influence of an object on a measurement. We will find a general formula that can be used in any geometry. The object-dependent parameters are calculated for objects that have slightly different optical parameters compared with those of the background, as well as for a completely black object. We will calculate the

sensitivity to both absorption and scattering. In Section 3 we will address the question of optimal boundaries. To do this, we need to describe the effects of boundaries and sources on the propagation of light. Subsequently, we can estimate the difference in sensitivities between the different kinds of boundaries. The theoretical results are compared with experiments. Finally, in Section 4 we present our conclusions.

## 2. PERTURBATION THEORY FOR GENERAL OBJECTS

Before we consider the influence of different boundaries, we first need to consider the sensitivity of a measurement for a given perturbation of the absorption and scattering parameters. Hence we need to determine what the difference in a measurement is between a homogeneous medium and a medium with some perturbation. The precise quantity that one measures depends on a lot of factors concerning the detector, among them its shape, surface area, and acceptance angle. In general, however, the measurement itself is proportional to the photon density at the detector position.<sup>3</sup> The photon density  $\Phi(\mathbf{r}, t)$  at position  $\mathbf{r}$  and at time  $t$  is described by the diffusion equation<sup>4</sup>

$$\frac{\partial}{\partial t} \Phi(\mathbf{r}, t) - \nabla \cdot D(\mathbf{r}) \nabla \Phi(\mathbf{r}, t) + v \mu_a(\mathbf{r}) \Phi(\mathbf{r}, t) = S(\mathbf{r}, t). \quad (1)$$

The absorption coefficient  $\mu_a$  and the transport scattering coefficient  $\mu_s$  can depend on the position in the medium. (We disregard the prime sometimes used to distinguish the transport scattering coefficient from the scattering coefficient itself.) The diffusion constant  $D = \frac{1}{3}v/\mu_s$  ( $v$  is the velocity of the light) then also depends on position. We do not take any absorption dependence of the diffusion constant into account, as many other authors do,<sup>2-6</sup> since corrections to  $D$  are of the same order as that of corrections to the diffusion equation itself.<sup>7-9</sup> For the diffusion equation to be valid, one needs<sup>4,5</sup>

$$\mu_a \ll \mu_s. \quad (2)$$

The source term  $S(\mathbf{r}, t)$  describes the density of photons generated per second. The diffusion equation (1) has to be supplemented with boundary conditions, which we will consider below.

Since the diffusion theory can handle only photon densities, then, without being able to distinguish different directions of propagation, we must take the source  $S$  to be isotropic. For simplicity we will consider only point sources. A short discussion on nonisotropic light sources will be given in Section 3, following Haskell *et al.*<sup>3</sup> When the source is amplitude modulated, the photon density will be time dependent, although always nonnegative. If we take only one Fourier component with frequency  $\omega$  into account, a source at position  $\mathbf{r}_s$  is then given by

$$S(\mathbf{r}, t) = S_\omega \exp(-i\omega t) \delta(\mathbf{r} - \mathbf{r}_s). \quad (3)$$

Unless  $\omega = 0$ , the corresponding photon density will be complex and have the same harmonic time dependence.

We will formulate the theory in terms of Green functions. A Green function describes the propagation of light in a homogeneous medium (no objects present), having only one source at an arbitrary position  $\mathbf{r}'$  (not necessarily the position  $\mathbf{r}_s$  of the physical source). From now on we will use  $\mu_a$  and  $\mu_s$  to characterize the homogeneous background medium and use extra subscripts to denote inhomogeneities. The Green function obeys the diffusion equation

$$-\nabla^2 G(\mathbf{r}, \mathbf{r}') + \kappa^2 G(\mathbf{r}, \mathbf{r}') = \delta(\mathbf{r} - \mathbf{r}'), \quad (4)$$

with the same boundary conditions as those for  $\Phi$ . Here  $\kappa = [(\mu_a v - i\omega)/D]^{1/2}$  is the inverse decay length of the background medium. For use below we also define  $\kappa_0 = \kappa(\omega = 0) = \sqrt{3\mu_a \mu_s}$ , which is real. We suppose that the solution to Eq. (4) is known. The photon density for the homogeneous medium is then given by

$$\Phi_0(\mathbf{r}) = (S_\omega/D) G(\mathbf{r}, \mathbf{r}_s). \quad (5)$$

The Green function obeys the symmetry of reciprocity,<sup>10</sup>

$$G(\mathbf{r}, \mathbf{r}') = G(\mathbf{r}', \mathbf{r}), \quad (6)$$

which can be useful in calculations.

An important Green function in our calculations is that of the infinite medium, given by

$$G_\infty(\mathbf{r} - \mathbf{r}_s) = (1/4\pi r) \exp(-\kappa r), \quad (7)$$

where  $r = |\mathbf{r} - \mathbf{r}_s|$  is the distance to the source. When  $\mathbf{r}$  and  $\mathbf{r}'$  are close together and far from boundaries, all Green functions tend to  $G_\infty$ . We will use this when we consider the influence of small objects.

### A. Born Series

For any source term  $S(\mathbf{r})$ , the solution to the homogeneous diffusion equation can be found as

$$\Phi(\mathbf{r}) = D^{-1} \int d\mathbf{r}' G(\mathbf{r}, \mathbf{r}') S(\mathbf{r}'). \quad (8)$$

Consider now the diffusion equation (1) at frequency  $\omega$ . Rewrite it such that the left-hand side corresponds to the homogeneous medium, and all terms that are due to perturbations of the optical parameters, as well as the physical source, are on the right-hand side:

$$\begin{aligned} -\nabla^2 \Phi(\mathbf{r}) + \kappa^2 \Phi(\mathbf{r}) &= \frac{S_\omega}{D} \delta(\mathbf{r} - \mathbf{r}_s) + \frac{\Delta D(\mathbf{r})}{D} \nabla^2 \Phi(\mathbf{r}) \\ &+ D^{-1} [\nabla D_{\text{obj}}(\mathbf{r})] \cdot [\nabla \Phi(\mathbf{r})] \\ &- 3\mu_s \Delta \mu_a(\mathbf{r}) \Phi(\mathbf{r}). \end{aligned} \quad (9)$$

Here we introduced the perturbation in the absorption constant and in the diffusion constant:

$$\Delta \mu_a(\mathbf{r}) = \mu_{a,\text{obj}}(\mathbf{r}) - \mu_a, \quad (10a)$$

$$\Delta D(\mathbf{r}) = D_{\text{obj}}(\mathbf{r}) - D, \quad (10b)$$

where the subscript obj is used to distinguish the parameters from the background. For the scattering parameter  $\Delta \mu_s$ , a similar relation holds. The complete right-hand side of Eq. (9) then acts as a source in Eq. (8). In general, one can therefore write the solution of the diffusion equation (after partial integration) as<sup>11,12</sup>

$$\begin{aligned}\Delta\Phi(\mathbf{r}) &\equiv \Phi(\mathbf{r}) - \Phi_0(\mathbf{r}) \\ &= -3\mu_s \int d\mathbf{r}' G(\mathbf{r}, \mathbf{r}') \Delta\mu_a(\mathbf{r}') \Phi(\mathbf{r}') \\ &\quad - \int d\mathbf{r}' [\nabla_{\mathbf{r}'} G(\mathbf{r}, \mathbf{r}')] \frac{\Delta D(\mathbf{r}')}{D} \nabla_{\mathbf{r}'} \Phi(\mathbf{r}').\end{aligned}\quad (11)$$

By substituting the expression for  $\Phi$  itself into the right-hand side and repeating this for every new expression, one generates a series. Each term in this Born series contains only  $\Phi_0$  and  $G$  (which are proportional) or derivatives thereof, but no longer the complete photon density  $\Phi$ . This (infinite) Born series is a solution of the diffusion equation for any spatial variation of the optical parameters.

For systems where the perturbation of  $\mu_s$  and  $\mu_a$  is small, one can use the first-order Born approximation, which implies that one replaces  $\Phi$  on the right-hand side of Eq. (11) by the most important contribution,  $\Phi_0$ . This is the basis of the forward calculation in many reconstruction techniques,<sup>11,13-17</sup> since it assumes that the measurements depend linearly on the perturbations.

## B. Small Objects

Let us now consider a single small object. For an object at position  $\mathbf{r}_o$  to be small, its characteristic size  $a$  must obey

$$a \ll |\mathbf{r}_o - \mathbf{r}_s|, |\mathbf{r}_o - \mathbf{r}|, |\kappa|^{-1}. \quad (12)$$

Outside the object the perturbations of the optical parameters vanish ( $\Delta\mu_a = \Delta D = 0$ ). Let us first consider only a perturbation in  $\mu_a$ , i.e.,  $\Delta D = 0$ . Since the object is small, the Green function  $G(\mathbf{r}, \mathbf{r}')$  in the integral of Eq. (11) is nearly constant and we find that

$$\Phi(\mathbf{r}) = \Phi_0(\mathbf{r}) - 3\mu_s G(\mathbf{r}, \mathbf{r}_o) \int_{\Omega} d\mathbf{r}' \Delta\mu_a(\mathbf{r}') \Phi(\mathbf{r}'), \quad (13)$$

where  $\Omega$  denotes the volume of the object. This still leads to a Born series. Every term of this series contains in the integral the photon density  $\Phi_0(\mathbf{r}') = S_{\omega} D^{-1} G(\mathbf{r}', \mathbf{r}_s)$ . Again, this Green function varies only little over the volume of the object. Therefore the photon density can be written as

$$\Phi(\mathbf{r}) = \Phi_0(\mathbf{r}) [1 + q Q(\mathbf{r}_o; \mathbf{r}, \mathbf{r}_s)], \quad (14)$$

where  $Q$  is the sensitivity for absorption<sup>2,18,19</sup> defined by

$$Q(\mathbf{r}_o; \mathbf{r}, \mathbf{r}_s) = \frac{4\pi}{\kappa_0} \frac{G(\mathbf{r}, \mathbf{r}_o) G(\mathbf{r}_o, \mathbf{r}_s)}{G(\mathbf{r}, \mathbf{r}_s)}. \quad (15)$$

The dependence of  $Q$  on  $\mathbf{r}$  has a banana shape.<sup>20</sup> The (real) factor  $4\pi/\kappa_0$  is conventional and has been chosen to make  $Q$  unitless and void of factors  $4\pi$  for the infinite medium. The rest of the Born series gives the strength  $q$  of the object:

$$\begin{aligned}q &= -\kappa_0 \frac{3\mu_s}{4\pi} \int_{\Omega} d\mathbf{r}' \Delta\mu_a(\mathbf{r}') \\ &\quad \times \left[ 1 - \frac{3\mu_s}{4\pi} \int_{\Omega} d\mathbf{r}'' \frac{\Delta\mu_a(\mathbf{r}'')}{|\mathbf{r}' - \mathbf{r}''|} (1 - \dots) \right].\end{aligned}\quad (16)$$

The usefulness of Eq. (14) [and similarly of Eq. (17) and relation (21) below] lies in the fact that the sensitivity for absorption  $Q$  depends not on the object but only on its position, and that the strength of the object,  $q$ , does not depend on geometrical factors of the surrounding medium. The strength does depend on the spatial distribution of the perturbation of the absorption coefficient, i.e., on the shape of the object and its absorption contrast with respect to the background. Since any measurement depends only on the position of the object and its strength, the shape of the object and the precise distribution of the absorption inside the object are therefore not important for the measurement. This means, for instance, that a very small and completely black object can give the same result as that for a larger object with only moderate absorption, as long as both fulfill condition (12). This has consequences for reconstruction, in the sense that not all characteristics of objects can be reconstructed. We will give the strength  $q$  of several objects in Subsection 2C.

We can give the same analysis for an object that has no extra absorption ( $\Delta\mu_a = 0$ ) but that has a different diffusion constant from that of the background. The description of scattering objects introduces the gradient of the Green functions [cf. Eq. (11)]. Since we have two of them, one for light going from source to object and one for light going from object to detector, we need a matrix  $p_{ij}$  with two indices to describe the object. In the same way as that above, we find that

$$\Phi(\mathbf{r}) = \Phi_0(\mathbf{r}) \left[ 1 + \sum_{i,j} p_{ij} P_{ij}(\mathbf{r}_o; \mathbf{r}, \mathbf{r}_s) \right]. \quad (17)$$

Here  $P_{ij}$  is the sensitivity for scattering:

$$P_{ij}(\mathbf{r}_o; \mathbf{r}, \mathbf{r}_s) = -\frac{4\pi}{\kappa_0^3} \frac{\nabla_{r_o,i} G(\mathbf{r}', \mathbf{r}_o) \nabla_{r_o,j} G(\mathbf{r}_o, \mathbf{r}_s)}{G(\mathbf{r}, \mathbf{r}_s)}. \quad (18)$$

Again, the factor  $-4\pi/\kappa_0^3$  is conventional. The object is characterized by the symmetric matrix

$$\begin{aligned}p_{ij} &= \frac{\kappa_0^3}{4\pi D} \int_{\Omega} d\mathbf{r}' \Delta D(\mathbf{r}') \left[ \delta_{ij} - \frac{1}{4\pi D} \sum_k \int_{\Omega} d\mathbf{r}'' \Delta D(\mathbf{r}'') \right. \\ &\quad \left. \times \nabla_{\mathbf{r}',i} \nabla_{\mathbf{r}'',k} \frac{1}{|\mathbf{r}' - \mathbf{r}''|} (\delta_{kj} - \dots) \right].\end{aligned}\quad (19)$$

For spherical symmetric objects the dipole term is a scalar:  $p_{ij} = p \delta_{ij}$ . In that case one needs not all elements of  $P_{ij}$  but only the trace:

$$\begin{aligned}P(\mathbf{r}_o; \mathbf{r}, \mathbf{r}_s) &= \sum_i P_{ii}(\mathbf{r}_o; \mathbf{r}, \mathbf{r}_s) \\ &= -\frac{4\pi}{\kappa_0^3} \frac{\nabla_{r_o} G(\mathbf{r}', \mathbf{r}_o) \cdot \nabla_{r_o} G(\mathbf{r}_o, \mathbf{r}_s)}{G(\mathbf{r}, \mathbf{r}_s)},\end{aligned}\quad (20)$$

which is the vector product of the gradients of two Green functions.<sup>2</sup> For objects with less symmetry, all components of  $p_{ij}$  can, in principle, be nonzero. But the deviation from the contribution  $p \delta_{ij}$  is generally small. Hence, in all the examples, we will use the simplified form (20).

A difference between absorbing objects described by Eq. (14) and scattering objects described by Eq. (17) is that

the former actually take light away, whereas the latter mainly redistribute the light, such that the total amount of light detected does not necessarily change. The description of objects that includes both scattering and absorption is somewhat more complex than that above. We will not address this problem here. We only note that strengths describing the combination of absorption and scattering are negligible when the object is also small with respect to the absorption and scattering lengths of the object itself, since such a combination is always a higher-order effect.

The next question to be asked is, what is the result for multiple objects? In first order all the different objects contribute linearly to the measurement. That is, for multiple objects, we can write

$$\Phi(\mathbf{r}) = \Phi_0(\mathbf{r}) \left[ 1 + \sum_o q_o Q(\mathbf{r}_o; \mathbf{r}_s, \mathbf{r}_d) + \sum_o p_o P(\mathbf{r}_o; \mathbf{r}_s, \mathbf{r}_d) \right], \quad (21)$$

where the index  $o$  identifies the objects. Equations (14) and (17) and relation (21) generalize the expressions given in Refs. 1, 2, and 21. We will see that the first-order approximation (21) is good, even when the difference between  $\Phi$  and  $\Phi_0$  is of the order of tens of percent. Note that relation (21) is basically the first-order Born approximation discussed in Subsection 2.A, but now with a more realistic description of single objects.

### C. Strength of Specific Objects

Now we will give the explicit form of the strengths  $q$  and  $p$  for different objects. Not many of them can be calculated analytically, however. For small objects and perturbations that are not too large, we again need only to take into account the first term of the series in Eqs. (16) and (19). For an object with volume  $\Omega$  and only a small constant perturbation in absorption,  $\Delta\mu_a$ , we find that

$$q = -\frac{\kappa_0^3 \Omega \Delta\mu_a}{4\pi\mu_a}, \quad p = 0, \quad (22)$$

and for an object with only a small constant perturbation in scattering,  $\Delta D$ , we find that

$$p = \frac{\kappa_0^3 \Omega \Delta D}{4\pi D}, \quad q = 0. \quad (23)$$

For spherical objects of radius  $a$ , one can find the results in Refs. 1 and 2 for general values of the optical parameters of the background and the object. For the specific case of  $\Delta\mu_a = 0$ ,  $\Delta D = D_{\text{obj}} - D$  is constant inside the spherical object, and for  $\kappa a \ll 1$ , these reduce to

$$p_{\text{sphere}} = (\kappa_0 a)^3 \frac{D_{\text{obj}} - D}{D_{\text{obj}} + 2D}. \quad (24)$$

One can show that the series in Eq. (19) gives the same result. Consequently, even for small radius  $a$ , one needs to take the full series into account when  $\Delta D$  itself is not small. When the scattering in the object increases,  $D_{\text{obj}}$  decreases, until  $p$  reaches a maximum value of  $-\frac{1}{2}(\kappa_0 a)^3$ . That  $p$  has a maximum is due to the fact that large scattering of the object implies that all the light will be re-

flected, almost at the point of entering. If this is so, the absolute amount of scattering given by the value of  $D_{\text{obj}}$  is no longer important. Also, the opposite case of a very transparent object, with large  $D_{\text{obj}}$ , leads to a saturation value of  $p = (\kappa_0 a)^3$ . We see that as long as  $D_{\text{obj}}$  and  $D$  differ enough, their precise values are not important for the determination of  $p$ .

We observe that for weak objects the strengths  $p$  and  $q$  scale with the volume of the object. One can use this to rewrite relation (21) into its integral equivalent<sup>12</sup>:

$$\Phi(\mathbf{r}) = \Phi_0(\mathbf{r}) \left[ 1 - \frac{3\mu_s \kappa_0}{4\pi} \int d\mathbf{r}_o \Delta\mu_a(\mathbf{r}_o) Q(\mathbf{r}_o; \mathbf{r}, \mathbf{r}_s) + \frac{3\kappa_0^3}{4\pi} \int d\mathbf{r}_o \frac{D_{\text{obj}}(\mathbf{r}_o) - D}{D_{\text{obj}}(\mathbf{r}_o) + 2D} P(\mathbf{r}_o; \mathbf{r}, \mathbf{r}_d) \right]. \quad (25)$$

For the case of  $\Delta D = 0$  and a large but constant  $\Delta\mu_a$  in the object ( $\kappa_{\text{obj}} a \geq 1$ ), one finds<sup>1,2</sup> that

$$q_{\text{sphere}} = -\kappa_0 a [1 - \tanh(\kappa_{\text{obj}} a) / \kappa_{\text{obj}} a], \quad p = 0. \quad (26)$$

In the limit of large absorption ( $\kappa_{\text{obj}} a \gg 1$ ), this leads to the strength of a black sphere:

$$q_{\text{black}} = -\kappa_0 a. \quad (27)$$

Note again that in the limit of large perturbations the precise value of the optical parameters of the object is no longer important. The strength (27) can also be found by solving the diffusion equation directly for a spherical object,<sup>20</sup> assuming that the photon density vanishes on the boundary of the object:

$$\Phi(|\mathbf{r} - \mathbf{r}_o| = a) = 0. \quad (28)$$

That this boundary condition is not exact is well known.<sup>3,4</sup> This is due to the approximate nature of the diffusion equation, which requires that  $\mu_a \ll \mu_s$  [cf. relation (2)]. This is not the case inside a strongly absorbing object. Equation (28) works rather well, however, when corrections to length scales of the order of the scattering length  $\mu_s^{-1}$  are negligible. For a small absorbing sphere, this is no longer the case, since  $a$  can be of the same order as  $\mu_s^{-1}$ . Therefore Eq. (27) no longer holds. In the neighborhood of an absorbing boundary, the photon density does not vanish. Instead, it has an offset. A boundary condition that incorporates this effect<sup>4</sup> and hence generally gives more accurate results<sup>3</sup> is (see also Section 3)

$$\Phi + \xi_{\text{ext}} \hat{\mathbf{n}} \cdot \nabla \Phi|_{\text{at the surface}} = 0. \quad (29)$$

Here  $\hat{\mathbf{n}}$  is a unit vector perpendicular to the surface of the scattering medium and pointing outward. The extrapolation length  $\xi_{\text{ext}}$  is of the order of  $\mu_s^{-1}$ . Its precise value depends on the ratio of refractive indices<sup>4,22-24</sup> [cf. Eq. (40) below] and on the geometry. Solving the diffusion equation (1) with a spherical object but using the boundary condition (29) instead of Eq. (28), one finds that

$$q_{\text{black}} = -\frac{\kappa_0 a^2}{a + \xi_{\text{ext}}}. \quad (30)$$

The length  $\xi_{\text{ext}}$  itself depends only weakly on  $a$ . For large  $a$  it takes the value of the semi-infinite medium<sup>4</sup>

$\xi_{\text{ext}} = 2/3\mu_s$ . In the limit of vanishing  $a$ , its value is  $\xi_a$  and will be calculated in the following.

Consider a virtual sphere of radius  $a \ll \mu_s^{-1}$ . We know that for a given source strength  $S_\omega$  (in photons per second) the photon density at the position  $\mathbf{r}_o$  of this sphere is given by  $\Phi_0(\mathbf{r}_o)$ . Within the diffusion approximation the photon flux is given by<sup>4</sup>  $I(\mathbf{r}, \hat{\mathbf{s}}) = (v/4\pi)(\Phi_0 - \mu_s^{-1}\hat{\mathbf{s}} \cdot \nabla\Phi_0)$ . The number of photons entering the sphere per unit of time,  $S_o$ , is given by this flux  $I$  times the cross section of the sphere,  $\pi a^2$ , integrated over all angles  $\hat{\mathbf{s}}$ , which results in  $S_o = \pi a^2 v \Phi_0$ . If the sphere is completely black,  $S_o$  denotes the number of photons absorbed by the sphere per unit of time. Hence the sphere acts as a negative source with strength  $S_o$ . The photon density can now be written as

$$\Phi(\mathbf{r}) = \Phi_0(\mathbf{r}) - (S_o/D)G(\mathbf{r}; \mathbf{r}_o). \quad (31)$$

Combining this with Eq. (14), we get  $q_{\text{black}} = -3\mu_s\kappa_0 a^2/4$  and consequently  $\xi_a = 4/3\mu_s$ , which is two times as large as  $\xi_{\text{ext}}$  for large  $a$ .

We see from Eq. (30) that a crossover exists in the dependence of  $q_{\text{black}}$  on the radius  $a$ , between small black spheres ( $a\mu_s < 1$ ) and larger spheres ( $a\mu_s > 1$ ). It is fair to ask if such a crossover exists for spheres that have only a small extra absorption compared with the background ( $\Delta\mu_a a \ll 1$ ). We know that for spheres that obey the diffusion equation (and therefore have relatively small  $\mu_a$ ) Eqs. (22) hold and hence  $q \sim a^3$ . For a very small sphere, we can use the same arguments as those above. The number of photons present is again  $4\pi\Phi_0(\mathbf{r}_o)a^3/3$ . The frequency at which these photons get absorbed in the sphere more than in the background is  $\Delta\mu_a v$ . Using again Eq. (31), we find that  $q = -a^3\Delta\mu_a\mu_s\kappa_0$  conforms to the first of Eqs. (22). We see that no crossover exists.

We can explain the cubic dependence on the radius  $a$  qualitatively as follows. For any  $a$  the number of photons entering the object is proportional to the number of photons absorbed if the object is perfectly black, i.e.,  $\propto q_{\text{black}}$  from Eq. (30). When  $a$  is small, this number scales with  $a^2$ . The average path length is linear in  $a$ . Consequently, the extra absorption that determines  $q$  is cubic in  $a$ . When  $a$  gets larger, the number of photons entering the sphere scales with  $a$ . The average length that a photon travels inside the sphere is then no longer linear in  $a$ : the photon will have a diffusive motion inside the sphere. Its average time in the sphere will be  $\sim a^2/D$ , and hence the average path length in the sphere will be  $\sim a^2\mu_s$ . Again, we find that  $q$  is cubic in  $a$ .

#### D. Example

Let us consider a simple situation to obtain some insight into the formulas, deriving the main dependencies on the parameters, as well as getting some feeling for the sensitivity to scattering and absorption. We take both the source and the detector at a distance  $r$  from the object, all three of them on a line. The sensitivities are then given by

$$Q = \frac{2}{\kappa_0 r}, \quad (32a)$$

$$P = \frac{2}{(\kappa_0 r)^3} (1 + \kappa r)^2. \quad (32b)$$

(Note the difference between the real  $\kappa_0$ , acting as a length scale, and the complex and frequency-dependent  $\kappa$ .) In many cases of practical interest for medical imaging, the distance  $r$  between source and object is of the same order as  $|\kappa|^{-1}$ . This means that both sensitivities are of equal order. For large  $r$  and zero frequency, they are even identical in this geometry. When taking a realistic spherical object, where  $q$  and  $p$  are given by Eqs. (22) and (24), we find the following for the perturbation in photon densities:

$$\frac{\Delta\Phi_q}{\Phi_0} = -\frac{\Delta\mu_a}{3\mu_a} (\kappa_0 a)^3 \frac{2}{\kappa_0 r}, \quad (33a)$$

$$\frac{\Delta\Phi_p}{\Phi_0} = \frac{\Delta D}{3D + \Delta D} (\kappa_0 a)^3 \frac{2}{\kappa_0^3 r^3} (1 + \kappa r)^2, \quad (33b)$$

where the index  $q$  ( $p$ ) denotes a perturbation in absorption (scattering). We see that, in general, the perturbation that is due to scattering can be as large as that which is due to absorption. In many cases of practical interest, however, the wavelength is chosen such that the mean absorption of normal tissue is at a minimum.<sup>25</sup> This means that any change in the tissue will result in a (large) increase in absorption, whereas the change in scattering will average out. This is used, for instance, in tissue oximetry.<sup>26</sup> Hence we expect that, in practice,  $\Delta\mu_a/\mu_a \gg \Delta D/D$ , so that for medical imaging purposes absorption is more important than scattering.

#### E. Amplitude-Modulated Sources

All formulas given above can be applied as well as to the case of an amplitude-modulated source. We will, as in the experiments, use the amplitude  $A$  and the phase  $\varphi$ , i.e.,

$$\Phi = A \exp(i\varphi), \quad (34)$$

and write  $\Phi_0 = A_0 \exp(i\varphi_0)$  for the homogeneous background medium. (For zero frequency  $\Phi$  itself is real, and hence  $\varphi = 0$ .) Consider a perturbation in the photon density, which we can write as

$$\Delta\Phi = |\Delta\Phi| \exp(i\vartheta). \quad (35)$$

From this perturbation one needs to calculate the perturbation in  $A$  and  $\varphi$ . For small perturbations we can write

$$\frac{\Delta A}{A_0} = |\Delta\Phi| \cos(\vartheta - \varphi_0)/A_0 = \text{Re}\left(\frac{\Delta\Phi}{\Phi_0}\right), \quad (36a)$$

$$\Delta\varphi = |\Delta\Phi| \sin(\vartheta - \varphi_0)/A_0 = \text{Im}\left(\frac{\Delta\Phi}{\Phi_0}\right). \quad (36b)$$

We give explicit formulas for the same example as that above, where the object is exactly in the middle between source and detector, both distances being equal to  $r$ . We get

$$\frac{\Delta A}{A_0} = \frac{2}{3} \left(\frac{a}{r}\right)^3 \left[ -\frac{\Delta\mu_a}{\mu_a} (\kappa_0 r)^2 + \frac{\Delta D}{3D + \Delta D} \text{Re}(1 + \kappa r)^2 \right], \quad (37a)$$

$$\Delta\varphi = \frac{2}{3} \left(\frac{a}{r}\right)^3 \frac{\Delta D}{3D + \Delta D} \text{Im}(1 + \kappa r)^2. \quad (37b)$$

In general, we see that the amplitude difference  $\Delta A/A_0$  is sensitive mostly to absorption inside the object, whereas the phase  $\Delta\varphi$  is sensitive mostly to the extra scattering of the object. When the object is not on the line between source and detector, the sensitivity has an extra exponential factor. Because of this factor both amplitude and phase can vary for a single object, even if it is purely absorbing or purely scattering with respect to the background.

### 3. OPTIMAL BOUNDARIES

#### A. Sources and Boundaries

The purpose of our research is to image an object inside some medium. This medium will, in general, be a finite one. It is well known that the boundary of the medium affects the measurements. One boundary of interest is the open boundary, where only air or a transparent fluid is surrounding the medium. For the description of the scattering of light inside the medium, this is almost equivalent to a complete black boundary, since no light that leaves the turbid medium will reenter it. An open boundary can also be accompanied by a mismatch in the refractive index between the turbid medium and the medium outside. An opposite kind of boundary is also possible, i.e., a boundary with as much reflection as possible, so that only a little amount of light gets lost. This can be done by surrounding the medium with mirrors. Surrounding the medium by another diffusive medium gives a similar result, since a diffusive medium also reflects much of the light entering it. The question arises, which of these two possibilities is better for imaging objects? In answering this question, we have to take into account both the sensitivity to the object, as discussed in Section 2, and the possible accuracy of the measurement, which benefits from large photon densities having less noise. Both change with boundary conditions. Also, the algorithm of reconstruction can favor a choice of boundaries. To study this problem, we will start with describing the boundaries and the way that we will treat them. Then we will look at both sensitivity and accuracy.

Typically, the source may consist of a fiber placed in the middle of a large medium or at the edge of the medium. Therefore the incoming light will be a directed beam of light with some aperture. The diffusion theory assumes point sources. It is possible to model a directed beam by a point source.<sup>3</sup> One has to determine where the model point source is located, given the physical source. Because of symmetry reasons this point source will be at some distance from the end of the fiber but on its axis  $\hat{\mathbf{n}}$ . This distance, which we will call  $\xi_{\text{in}}$ , will depend on the aperture. It has been shown<sup>27</sup> that for a collimated beam having a small aperture,  $\xi_{\text{in}} = \mu_s^{-1}$  is a reasonable choice. We will take this value in the following. Larger apertures will have smaller  $\xi_{\text{in}}$ . It is known that the diffusion theory gives inaccurate results close to boundaries. To use the diffusion theory, it is therefore advantageous to have a (model) source as deep into the medium as possible. This means that when the system is to be described by a diffusion equation, a small aperture of a source at the boundary would be best.

When we model a physical detector, the same argument as that above holds. The physical detector also consists of a fiber. We assume that it has a small aperture, too. Because of the symmetry with respect to the source fiber, the intensity detected in this way will be proportional to the photon density a length  $\xi_{\text{in}}$  away from this detector. This symmetry between source and detector is a result of reciprocity<sup>10</sup> [cf. Eq. (6)]. There is another way of looking at this. The approximation that one makes in deriving the diffusion equation from the theory of radiative transfer is to write the photon flux  $I(\mathbf{r}, \hat{\mathbf{s}})$  at position  $\mathbf{r}$  in the direction  $\hat{\mathbf{s}}$  as<sup>4</sup>

$$I(\mathbf{r}, \hat{\mathbf{s}}) = \frac{v}{4\pi} [\Phi(\mathbf{r}) - \mu_s^{-1} \hat{\mathbf{s}} \cdot \nabla\Phi] \approx \frac{v}{4\pi} \Phi(\mathbf{r} - \mu_s^{-1} \hat{\mathbf{s}}). \quad (38)$$

The flux at the detector position and pointing into the fiber is then

$$I(\mathbf{r}_d, -\hat{\mathbf{n}}) \approx \frac{v}{4\pi} \Phi(\mathbf{r}_d + \xi_{\text{in}} \hat{\mathbf{n}}), \quad (39)$$

which is proportional to the photon density a length  $\xi_{\text{in}} = \mu_s^{-1}$  in front of the physical detector.

Apart from the sources, we need to model boundaries as well. This can be done by the boundary condition (29).<sup>3,4,22,28</sup> This boundary condition can be derived by using conservation of light flux at the boundary in combination with the requirement that no light enter the medium. (Note that sources at physical boundaries are modeled as point sources in the medium and therefore do not interfere with these boundary conditions.) The value of  $\xi_{\text{ext}}$  is given by<sup>5,22</sup>

$$\xi_{\text{ext}} = \frac{2}{3\mu_s} \frac{1 + 3 \int_0^{\pi/2} d\theta R(\theta) \sin \theta \cos^2 \theta}{1 + 2 \int_0^{\pi/2} d\theta R(\theta) \sin \theta \cos \theta}, \quad (40)$$

where  $R(\theta)$  is the reflectivity of the boundary for light incident at an angle  $\theta$ . However, the boundary condition (29) is not always easy to handle. For small  $\xi_{\text{ext}}$  one can expand  $\Phi$  around its value at the boundary  $\mathbf{r}_b$ . With use of the boundary condition (29), this results in  $\Phi(\mathbf{r}) \approx (\mathbf{r} - \mathbf{r}_b - \xi_{\text{ext}} \hat{\mathbf{n}}) \cdot \nabla\Phi(\mathbf{r}_b)$ . Hence the photon density vanishes for  $\mathbf{r} = \mathbf{r}_b + \xi_{\text{ext}} \hat{\mathbf{n}}$ , i.e., at a distance  $\xi_{\text{ext}}$  outside the medium. This is basically the requirement of the so-called extrapolated boundary<sup>4,23,24</sup>: the density is extrapolated by a distance  $\xi_{\text{ext}}$  beyond the boundaries, at which point the photon density vanishes, i.e.,

$$\Phi[(\mathbf{r} - \mathbf{r}_b) \cdot \hat{\mathbf{n}} = \xi_{\text{ext}}] = 0. \quad (41)$$

This simplification of the boundary condition can be done only when the photon density is approximately linear over a distant  $\xi_{\text{ext}}$ ; consequently, the extrapolated-boundary condition can be used only for  $\kappa \xi_{\text{ext}} \ll 1$ . This puts a restriction on the use of Eq. (41). It is, however, much simpler to handle than Eq. (29) in calculating the photon density, and it therefore has been used extensively

in the literature. Haskell *et al.*<sup>3</sup> showed that the difference between both boundary conditions is indeed small for reasonable optical parameters. We prefer to use the latter boundary condition [Eq. (41)] whenever possible.

The extrapolation length  $\xi_{\text{ext}}$  used in Eqs. (29) and (41) depends on the refractive-index mismatch between the scattering medium and its surroundings.<sup>22</sup> It is of the order of a mean free path. It has a minimum of  $2/3\mu_s$  for the semi-infinite geometry<sup>4</sup> (its value when considering the theory of radiative transfer<sup>29</sup> is  $0.71\mu_s^{-1}$ ). It increases with refractive-index mismatch and can become several mean free paths long.<sup>23,24</sup> Hence we can model the amount of Fresnel reflection at the boundary, which is due to this mismatch, by the value of  $\xi_{\text{ext}}$ .

The introduction of  $\xi_{\text{ext}}$  enlarges the system effectively with a distance of the order of the mean free path. One would therefore expect only a small correction to the results, of the order of  $\xi_{\text{ext}}/L$ , where  $L$  is a measure of the system size. This is, however, not true in the case where either source or detector is close to a boundary. The less deep the source is located, the larger the losses at the boundary will be, and consequently the smaller the transmission will be, for example. As we will see, for small  $\xi_{\text{ext}}$  the photon density scales with the distance between the (model) source and the boundary of the effective medium:  $\xi \equiv \xi_{\text{ext}} + \xi_{\text{in}}$ . When the absolute value of the photon density is calculated, the value of  $\xi_{\text{ext}}$  is important. The source strength  $S_\omega$  is of equal importance. Fresnel reflection at the boundary has its influence both on the source term and on the value of  $\xi_{\text{ext}}$ . Since it is, in practice, difficult to determine the source term, we will seek quantities that depend only on relative measurements. For these cases the exact value of  $\xi_{\text{ext}}$  is not very important as long as  $\kappa\xi_{\text{ext}}$  is small. For reflecting boundaries, however,  $\kappa\xi_{\text{ext}}$  can be large, in which case the value of  $\xi_{\text{ext}}$  is important.

We want to study the influence of the boundary extrapolation. Two limits are evident. The first is the limit  $\xi_{\text{ext}} \rightarrow \infty$ . In this limit the two boundary conditions (29) and (41) give different results. The former corresponds to having perfect mirrors at the boundaries, reflecting all the light. The latter corresponds to an infinite medium. Both are similar but not equivalent. The second limit is that of small  $\xi_{\text{ext}}$ . This is almost equivalent to completely absorbing boundaries, or a (large) surrounding medium that does not scatter the light and that has (almost) matching refractive index. Both will be considered. When considering good reflecting mirrors, we assume that measurements are made by using small fibers, which penetrate the mirrors, instead of measuring the small amount of light that is transmitted through the mirrors.

## B. Green Functions

To determine the sensitivities  $Q$  and  $P$  and their dependence on the boundary, we first need to calculate the Green functions.<sup>30</sup> We will start with a semi-infinite medium, since this is the simplest case and it already gives some insight. The medium occupies the half-space  $z > 0$ . The source is, as above, located at  $\mathbf{r}_s$ . The difference in the  $x$ - $y$  plane between the position and the source is given by the vector  $\boldsymbol{\rho} = \mathbf{r} - \mathbf{r}_s$ . The system is

cylindrically symmetric, so that the Green function and other resulting quantities depend only on  $\rho = |\boldsymbol{\rho}|$  and not on the direction of  $\boldsymbol{\rho}$ . We find it useful to perform a Fourier transform in the  $x$ - $y$  plane, writing

$$\begin{aligned} G_s(\boldsymbol{\rho}, z, z_s) &= \int \frac{d^2\mathbf{q}}{(2\pi)^2} \exp(i\mathbf{q} \cdot \boldsymbol{\rho}) G_s(\mathbf{q}, z, z_s) \\ &= \int_{\kappa}^{\infty} \frac{d\alpha}{2\pi} J_0(\rho\sqrt{\alpha^2 - \kappa^2}) \alpha G_s(\alpha; z, z_s). \end{aligned} \quad (42)$$

The subscript  $s$  stands for semi-infinite, and  $J_0$  is a Bessel function. The change to the variable  $\alpha^2 = \kappa^2 + \mathbf{q}^2$  is introduced for later convenience. For amplitude-modulated sources,  $\kappa$  and therefore  $\alpha$  will be complex. However, for notational simplicity we will write the integral over  $\alpha$  as being from  $\kappa$  to  $\infty$ . To find the Green function, we need to solve Eq. (4). After Fourier transformation we get

$$\left( -\frac{\partial^2}{\partial z^2} + \alpha^2 \right) G_s(\alpha; z, z_s) = \delta(z - z_s). \quad (43)$$

Since we do not want to restrict the value of  $\xi_{\text{ext}}$  yet, we will use the boundary condition (29). The solution for the Green function at fixed  $\alpha$  is then given by

$$\begin{aligned} G_s(\alpha; z, z_s) &= \frac{1}{2\alpha} \left[ \exp(\alpha z_{\min}) - \frac{1 - \alpha\xi_{\text{ext}}}{1 + \alpha\xi_{\text{ext}}} \right. \\ &\quad \left. \times \exp(-\alpha z_{\min}) \right] \exp(-\alpha z_{\max}), \end{aligned} \quad (44)$$

as can be checked by substitution. We defined  $z_{\min} = \min(z, z_s)$  and  $z_{\max} = \max(z, z_s)$ . The Green function in real space is then given by

$$\begin{aligned} G_s(\boldsymbol{\rho}, z, z_s) &= \int_{\kappa}^{\infty} \frac{d\alpha}{4\pi} J_0(\rho\sqrt{\alpha^2 - \kappa^2}) \\ &\quad \times \left[ \exp(\alpha z_{\min}) - \frac{1 - \alpha\xi_{\text{ext}}}{1 + \alpha\xi_{\text{ext}}} \right. \\ &\quad \left. \times \exp(-\alpha z_{\min}) \right] \exp(-\alpha z_{\max}). \end{aligned} \quad (45)$$

Equation (7) for the Green function  $G_\infty$  in the infinite medium can be found from Eq. (45) by considering a source and a final position far into the medium ( $\kappa z_{\min} \gg 1$ ). Then the boundary will not have any influence, and we find that

$$\begin{aligned} G_\infty(\boldsymbol{\rho}, z, z_s) &= \int_{\kappa}^{\infty} \frac{d\alpha}{4\pi} J_0(\rho\sqrt{\alpha^2 - \kappa^2}) \\ &\quad \times \exp[-\alpha(z_{\max} - z_{\min})] \\ &= \frac{1}{4\pi} \exp(-\kappa r), \end{aligned} \quad (46)$$

where  $r^2 = \rho^2 + (z - z_s)^2$ . Using this equality, one can rewrite the Green function (45) for the semi-infinite medium as<sup>3</sup>

$$G_s(\rho, z, z_s) = \frac{1}{4\pi r} \exp(-\kappa r) + \frac{1}{4\pi r_+} \exp(-\kappa r_+) - \frac{2}{\xi_{\text{ext}}} \int_{-\infty}^{-z_s} dz' \frac{1}{4\pi r'} \exp(-\kappa r') \times \exp[(z' + z_s)/\xi_{\text{ext}}], \quad (47)$$

where  $r_+^2 = \rho^2 + (z + z_s)^2$  and  $r'^2 = \rho^2 + (z - z')^2$ . This expression can be interpreted as follows. The first term is the result from the original source, when no boundaries are present. The second term describes the propagation of light from a source just on the other side of the physical boundary at  $z = 0$ , which we call the mirror source. The last term describes the propagation of light from a distribution of sources on the  $z$  axis between  $z' = -\infty$  and  $z' = -z_s$ . The density of this distribution is a Poisson distribution  $\xi_{\text{ext}}^{-1} \exp[(z' + z_s)/\xi_{\text{ext}}]$  and has a total strength of  $-2$ .

We can now model the different boundaries by taking the limiting values of  $\xi_{\text{ext}}$ . For perfectly reflecting boundaries ( $\xi_{\text{ext}} \rightarrow \infty$ ), the distribution of sources at  $z'$  has a vanishing contribution for any position. Hence the Green function has only two terms, that of the original source and that of the mirror source.

If we take the other limit,  $\xi_{\text{ext}} \rightarrow 0$ , the distribution term is limited to the one point  $z' = -z_s$ . The Green function then consists of a term describing the propagation from the original source and a term describing the propagation from the mirror source, but with total strength  $-1$ . For  $\xi_{\text{ext}} = 0$  the Green function itself vanishes at the boundary, whereas for  $\xi_{\text{ext}} \rightarrow \infty$  its derivative with respect to  $z$  vanishes. This can also be seen directly from the boundary condition (29). Note that for a realistic absorbing boundary the value of  $\xi_{\text{ext}}$  does not vanish completely. For small values we can write Eq. (44) as

$$G_s(\rho, z, z_s) = G_\infty(\sqrt{(z - z_s)^2 + \rho^2}) - G_\infty(\sqrt{(z - z_s - 2\xi_{\text{ext}})^2 + \rho^2}), \quad z > z_s. \quad (49)$$

For large but finite  $\xi_{\text{ext}}$ , it is not possible to find an expression such that the Green function or its derivative vanishes at the same position for every  $\alpha$ . Therefore no extrapolated boundary in any sense can be used for good but not perfect mirrors. Qualitatively, a mirror that is not perfectly reflecting can be described by using a mirror source of a somewhat smaller strength. For quantitative calculations, however, one needs to use the full expression (47).

The next geometry that we consider is that of the slab. The slab geometry consists of a medium of infinite extent in both the  $x$  and  $y$  directions, but limited between two boundaries in the  $z$  direction:  $0 < z < L$ . In a slab geometry two qualitatively different measurements are possible. The first is a reflection measurement, which is similar to a reflection measurement for a semi-infinite medium. The second is a transmission measurement, where source and detector are on two opposite boundaries. Also, for other (finite) geometries that have smooth and convex boundaries (such that without scattering every detector can see all possible sources), any measurement is either like a reflection measurement or like a transmission measurement. For our discussion it suffices to consider these two possibilities as general prototypes.

As we did for the semi-infinite medium, we take the physical source at  $z = 0$ , pointing into the medium. We then need to solve Eq. (44) to find the Green function. The boundary condition (29) takes the explicit form

$$G_L(0, z_s) = \xi_{\text{ext}} \partial_z G(z, z_s)|_{z=0}, \quad (50a)$$

$$G_L(L, z_s) = -\xi_{\text{ext}} \partial_z G(z, z_s)|_{z=L} \quad (50b)$$

for the slab geometry considered here. We find that

$$G_L(\alpha; z, z_s) = \frac{[\exp(\alpha z_{\text{min}}) - F \exp(-\alpha z_{\text{min}})]\{\exp[\alpha(L - z_{\text{max}})] - F \exp[-\alpha(L - z_{\text{max}})]\}}{2\alpha[\exp(\alpha L) - F^2 \exp(-\alpha L)]}, \quad (51a)$$

$$F = \frac{1 - \alpha \xi_{\text{ext}}}{1 + \alpha \xi_{\text{ext}}}. \quad (51b)$$

$$G_s(\alpha; z, z_s) = \frac{1}{2\alpha} \{\exp(\alpha z_{\text{min}}) - \exp[-\alpha(z_{\text{min}} + 2\xi_{\text{ext}})]\} \times \exp(-\alpha z_{\text{max}}), \quad \kappa \xi_{\text{ext}} \ll 1. \quad (48)$$

This expression and the resulting Green function  $G(\rho, z, z_s)$  again describe two sources, one at the original source position and one (with strength  $-1$ ) at  $-z_s - 2\xi_{\text{ext}}$ . The Green function then indeed vanishes at the extrapolated boundary  $z = -\xi_{\text{ext}}$ , according to the boundary condition (41). In real space the resulting Green function is given by<sup>31</sup>

The Green function in real space is then given by

$$G_L(\rho, z, z_s) = \int_{\kappa}^{\infty} \frac{d\alpha}{4\pi} J_0(\sqrt{\alpha^2 - \kappa^2} \rho) 2\alpha G_L(\alpha; z, z_s). \quad (52)$$

Expression (52) can be simplified when we can make use of the boundary condition (41) instead of the boundary condition (29). This results again in the use of mirror sources.<sup>32</sup> In the slab geometry the system consists of two extrapolated boundaries, where the photon density has to vanish. To find the Green function, one needs a mirror source for each of these two boundaries. Each

mirror source also needs its own image in both boundary planes, which in turn need their own images. This leads to an infinite number of mirror sources, all regularly spaced. The formula for the Green function  $G_L$  of the slab then reads as<sup>33</sup>

$$G_L(\mathbf{r}, \mathbf{r}_s) = \sum_{m=-\infty}^{\infty} [G_{\infty}(\mathbf{r}, \mathbf{r}_s + 2m(L + 2\xi_{\text{ext}})\hat{\mathbf{z}}) - G_{\infty}(\mathbf{r}, \sigma_z \mathbf{r}_s - 2\xi_{\text{ext}}\hat{\mathbf{z}} + 2m(L + 2\xi_{\text{ext}})\hat{\mathbf{z}})]. \quad (53)$$

Here  $\sigma_z$  is a mirror operation in the  $x$ - $y$  plane:  $\sigma_z \mathbf{r} = \sigma_z(x, y, z) \equiv (x, y, -z)$ .

### C. Reflecting Boundaries

We now consider the differences between an infinite medium and a medium bounded by mirrors. As mentioned in Subsection 3.B, the Green function consists of only two terms, that of the original source and that of the mirror source. Suppose that the source is at a boundary, which we model with  $z_s = \xi_{\text{in}} = \mu_s^{-1}$ . Then the source and its mirror image are separated by a distance of  $2\mu_s^{-1}$ . For positions not too close to the source, the mirror source will appear as strong as the original source (the difference being a factor of the order of  $\kappa/\mu_s$ , or  $1/\mu_s r$  smaller). Hence

$$G_s(\rho, z, \xi_{\text{in}}) \approx 2G_{\infty}(\rho, z, \xi_{\text{in}}), \quad \xi \rightarrow \infty. \quad (54)$$

This enhancement appears for every position  $\mathbf{r}$ , and therefore the Green function from source to detector at the same boundary is enhanced by a factor of 2. The Green function from source to object, well away from a boundary, is also enhanced. For symmetry reasons the Green function from object to detector is enhanced by the same factor. Bearing in mind the definition (15) of the sensitivity for absorption, we see that this sensitivity itself also gets enhanced by a factor of 2 for the measurement in reflection described here:

$$Q_{\text{mirror}} \approx 2Q_{\infty} \quad (\text{reflection experiment}). \quad (55)$$

Next we consider a transmission experiment. The Green functions from source to object and from object to detector get enhanced by a factor of 2 with respect to the Green function of the infinite medium, as above. The Green function from source to detector gets an enhancement factor of 2, which is due to the mirror close to the source. The mirror at the detector, however, is not the same mirror. Hence, for symmetry reasons alone, at the detector we also get an enhancement of 2. The total enhancement for the Green function from source to detector is then 4. For the sensitivity to absorption  $Q$ , we then find that

$$Q_{\text{mirror}} \approx Q_{\infty} \quad (\text{transmission experiment}). \quad (56)$$

Another way of looking at this is by using a mirror object instead of mirror sources and detectors. One can then easily see that in reflection one actually measures two objects, one on each side of the boundary, one of them a mirror object. In transmission the mirror objects will be too far from either source or detector to be measured. Corrections to this simple picture have to be made when

the system size  $L$  is such that  $\exp(-\kappa L) \approx 1$  or when the object is close to a boundary. In the former case one needs the full expression for the Green function in a slab geometry [Eq. (52)]. When the object is close to a boundary but far from both source and detector, the ratio between  $Q_{\text{mirror}}$  and  $Q_{\infty}$  is again 2.

A mirror that is almost perfectly reflecting can be described qualitatively by a mirror source of a somewhat smaller strength than 1. The enhancement factors discussed above become smaller than 2 but are still present. For mirrors reflecting only a part of the light, the value of  $\xi_{\text{ext}}$  decreases even more. In those cases there is even less difference between an infinite medium and a bounded medium. The Green function in the infinite medium is such that  $\Phi \approx \kappa^{-1}|\nabla\Phi|$ . Therefore the boundary condition (29) is almost fulfilled by  $G_{\infty}$  when  $\kappa\xi_{\text{ext}} \approx 1$ . For boundaries that are even less reflecting—we will show experimental examples of this in Subsection 3.D—the sensitivity is somewhere between that of an infinite medium and that of a medium with absorbing boundaries. These different boundaries will be compared in specific geometries below. We can conclude that the influence of mirrors on the Green function is a factor only of the order of 1 with respect to the infinite system.

The arguments presented above also hold for the sensitivity to scattering  $P$ . Since the difference between an infinite system and a system with good mirrors is a factor only between 1 and 2, we can conclude that a boundary with good mirrors is qualitatively equivalent to an infinite system:

$$Q_{\text{mirror}} \approx Q_{\infty}, \quad P_{\text{mirror}} \approx P_{\infty}, \quad (57)$$

the difference being a factor only of the order of 1.

For black boundaries the situation is entirely different. For small  $\xi_{\text{ext}}$  the source and its mirror have different signs. Hence the difference between these two sources determines the Green function. Instead of  $G_{\infty}$  itself, its derivative becomes important. In this case there will also be differences between the sensitivities for absorption and for scattering. It is difficult to compare the sensitivities for absorbing boundaries with those of an infinite medium by using only general principles, as above. For the case of absorbing boundaries, we will do some explicit calculations in Subsection 3.E. Before we do this, however, we first describe the experimental results.

### D. Experimental Results

The experimental setup to measure the influence of various kinds of boundaries on the detectability of objects is as follows: As a turbid medium a fish tank filled with 1% INTRALIPID is used. INTRALIPID is an emulsion of soybean oil in water, commercially available in concentrations of 10% and 20%. We diluted the 10% solution ten times to obtain a transport scattering coefficient of  $\mu_s = 0.85 \text{ mm}^{-1}$  and an absorption coefficient of  $\mu_a = 7 \times 10^{-4} \text{ mm}^{-1}$ , resulting in  $\kappa_0 = 0.042 \text{ mm}^{-1}$ . The light from a temperature-stabilized semiconductor laser operating at 670 nm is administered by a multimode fiber with a diameter of 1 mm. The light intensity at the fiber end in the fish tank is approximately 1.2 mW. The detector position is determined by one end of a second multimode fiber, which is connected at the other end to a

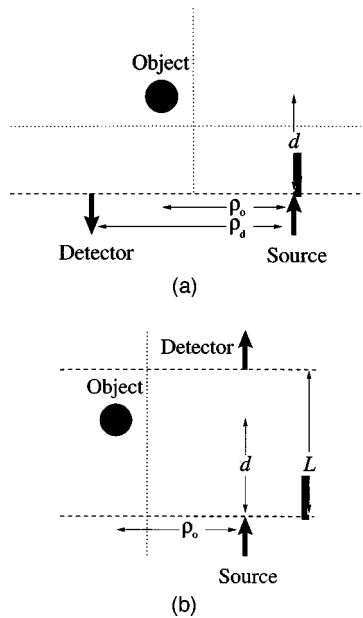


Fig. 1. Schematic view of the geometry used for experiments and theory. (a) For measurements in reflection, the source-detector distance in the  $x$ - $y$  plane is denoted by  $\rho_d$ . The position of the object is given by its lateral coordinate  $\rho_o$  and its depth  $d$ . The dashed line shows the position of the physical boundary when present. The object is moved along the horizontal dotted line for the measurements of Figs. 2 and 4 below and along the vertical dotted line for the measurements of Figs. 3 and 5. The scale of the object corresponds to the black cylinder. (b) For measurements in transmission,  $L$  is the thickness of the slab in the  $z$  direction. The position of the object is given by  $\rho_o$  and  $d$ . The dashed lines show the position of the physical boundaries when present. The object is moved along the vertical dotted line for the measurements of Figs. 6 and 7.

Hamamatsu H5783-01 photomultiplier, having a maximum sensitivity of  $3 \times 10^3$  A/W at 670 nm. An electrometer measures directly the current output of the photomultiplier, and after analog-to-digital conversion the data are archived in a computer. The source and detector fibers are positioned in the fish tank, either with small white Delrin holders to resemble an infinite medium, in the 1-mm holes of black Perspex plates, or in the holes of polished aluminum plates acting as reflecting boundaries.

Both absorbing as well as scattering objects are studied. The absorbing object is a 5-mm-diameter cylinder made of black Delrin with a height of 5 mm. A computer-controlled stepper motor holding a 2-mm-diameter white Delrin rod attached to the cylinder makes it possible to move the object freely through the fish tank. The rod has a negligible influence in comparison with that of the black cylinder. The scattering object is a hollow white Delrin cylinder with an internal diameter of 8.4 mm (wall thickness 0.5 mm) and an effective height of 55 mm, filled with 20% INTRALIPID. To correct for any absorbing effects of this container, each measurement is followed by a second one in which the container is filled with the same concentration as that of the surrounding medium, i.e., 1% INTRALIPID. Only the differences between two such scans are displayed in the figures.

In Fig. 1(a) we show the geometry for the measurements in reflection (we discuss the experiments in transmission below). We performed two measurements. For

both we have taken a fixed source-detector distance  $\rho_d = 30$  mm. The object is then scanned either parallel to the source-detector line, with constant  $d$ , or over the symmetry line  $\rho_o = \rho_d/2$ , with varying  $d$ . For all situations we have measured the signal with and without an object. The difference is then normalized by the measured signal without the object, which equals the ratio of photon densities,  $\Delta\Phi/\Phi_0$ .

To compare the experimental results with theory, we used Eqs. (15) and (20) to calculate the sensitivities  $Q$  and  $P$ . The Green functions that we used are Eq. (7) for the infinite medium, Eq. (49) for the semi-infinite medium with absorbing boundaries, Eq. (47) for the semi-infinite medium with reflecting boundaries, and Eq. (52) for the slab. For the absorbing cylinder we took the value of  $Q$  at the center point of the object and multiplied it by  $q$  to find  $\Delta\Phi_q/\Phi_0$ . Since the scattering object is large, we cannot use the value of  $P$  at only one point. Instead, we use Eq. (25) to find  $\Delta\Phi_p$ , with  $D/D_{obj} = 20$ . For comparison below we calculate the strength as if it were a small object and find that  $p = -0.025$ .

To determine  $q$ , we use Eq. (30) for  $q_{black}$ , with an effective radius  $a$ . We determine  $a$  by assuming that it is such that the surface of the effective sphere,  $4\pi a^2$ , equals the surface of the cylinder,  $\pi d(h + d/2)$ . The reason for taking the surface is that  $q$  scales approximately with  $a^2$ . We find that  $a = 3.06$  mm. Since this is already larger than a mean free path, we choose for  $\xi_{ext}$  its value for large  $a$ , which is  $0.67\mu_s^{-1} = 0.79$  mm. We find that  $q = -0.10$ .

The different boundaries are characterized by the value of the extrapolation length  $\xi_{ext}$ , as defined in Eq. (40). For the black boundaries we find that  $\mu_s \xi_{ext} = 0.67$ . For the aluminum plates, having a refractive index of  $1.4 - 6.28i$  (reflection for normal incidence of 88%), we use  $\mu_s \xi_{ext,Al} = 7.34$ . For a theoretical comparison we also calculated the results for a gold-coated mirror, with a refractive index of  $0.134 - 3.65i$  (reflection for normal incidence of 96%), and hence  $\mu_s \xi_{ext,Au} = 28.0$ .

In Fig. 2 we show the results for the sensitivity to the

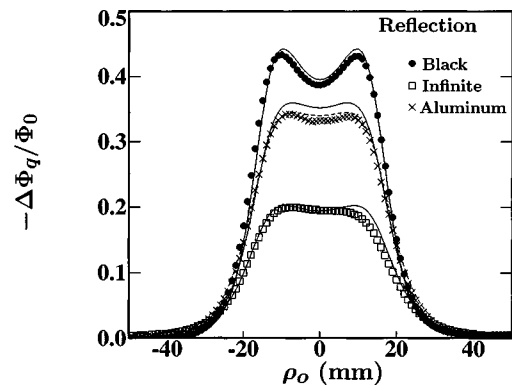


Fig. 2. Sensitivity to absorption  $\Delta\Phi_q/\Phi_0 = qQ$  in a reflection measurement as a function of the lateral position  $\rho_o$ . The source-detector distance  $\rho_d$  is 30 mm. The depth  $d$  of the object is 10 mm. Squares, an infinite medium; crosses, a semi-infinite medium with reflecting aluminum boundaries; dots, a semi-infinite medium with absorbing boundaries. The solid curves are the corresponding theoretical curves; the dashed curve is the theoretical curve for a reflecting gold mirror.

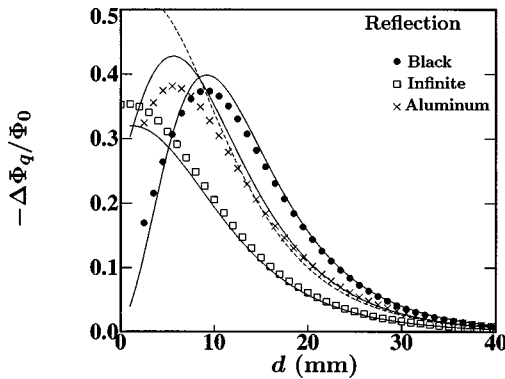


Fig. 3. Sensitivity to absorption  $\Delta\Phi_q/\Phi_0 = qQ$  in a reflection measurement. The parameters are the same as those in Fig. 2, but now the lateral distance  $\rho_o$  is fixed at  $\rho_d/2 = 15$  mm and the depth  $d$  is varied.

absorbing object. The scan is parallel to the line joining the source and the detector. The three sets of data show the measurements for an infinite medium and for a semi-infinite medium with either absorbing or reflecting (aluminum) boundary. The corresponding theoretical results are shown with solid curves. The two maxima are at positions  $\rho_o$  such that the object is in front of either source or detector. The correspondence between experiment and theory is good, even though up to 45% of the light is already absorbed by the object. Remember that the theory is based on the assumption of small objects. This does not mean, however, that only small  $\Delta\Phi/\Phi_0$  can be described; larger values can be considered, as long as the strength  $q$  is calculated from the full expression in Eq. (16). No adjustable parameters have been used. The dashed theoretical curve is for a semi-infinite reflecting (gold) boundary, which has a higher reflectivity than that of the aluminum boundary. For the same source-detector distance, we also scanned the object over the symmetry line  $\rho_o = \rho_d/2$ . The results are plotted in Fig. 3. Again, the correspondence is quite good.

We note that the sensitivity  $Q$  is proportional to the data in the figures. One can see in Figs. 2 and 3 that, in general, the sensitivity for the semi-infinite medium with absorbing boundaries will be larger than that for the semi-infinite medium with reflecting boundaries or than that of the infinite medium. This is not true for objects close to absorbing boundaries, where the amount of light is small. The sensitivity  $Q$  of the semi-infinite medium with reflecting boundaries seems to be between that of the two other cases. As mentioned above, this results from the fact that the aluminum mirrors reflect an amount of light that is between that of the absorbing boundary and of that part of the infinite medium that is on the other side of the dashed curve in Fig. 1. The dashed curve shows a sensitivity that is proportional to the sensitivity in the infinite medium, as described by relation (55). For  $d \geq 10$  mm the difference between a good mirror (dashed curve) and a not-so-good mirror (crosses, solid curve) is minimal. (The exact curves depend on the values of  $\xi_{\text{ext}}$ .) Although the Green function, in general, increases when the reflection of the boundary increases, the sensitivity, involving three Green functions, has a behavior that is different. When the object is

close to the boundary, the sensitivity for an aluminum mirror drops, since the amount of light near the boundary is low. For the gold mirror the sensitivity keeps rising and will be maximal at the boundary itself. Therefore the difference between a good mirror and a not-so-good mirror is visible mainly close to boundaries, at least for reflection experiments.

We also measured the sensitivity for scattering  $P$ . The results are shown in Figs. 4 and 5 for the same geometries as those in Figs. 2 and 3, respectively. The data points are for an infinite medium and a medium with absorbing boundaries. The theoretical curves again correspond to the data points. Systematic errors include the determination of the position of the scattering object and the drift of the detector during the measurement. As a result of the subtraction of two measurements, these small errors lead to larger errors in the determination of  $\Delta\Phi_p$ . The final error is equivalent to an error of the order of 1 mm, which is already large enough to explain the discrepancies between theory and experiment. Note that the shape of the curves agrees quite well with that from theory.

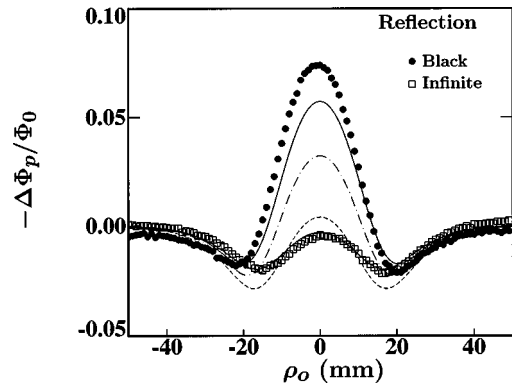


Fig. 4. Sensitivity to scattering  $\Delta\Phi_p/\Phi_0$  in a reflection measurement as a function of the lateral position  $\rho_o$ , with  $\rho_d = 30$  mm, as in Fig. 2. Squares, infinite medium ( $d = 15$  mm); dots, semi-infinite medium with absorbing boundaries ( $d = 17$  mm). The solid curves are the corresponding theoretical curves; the dotted-dashed curve is the theoretical curve for the aluminum mirror; the dashed curve is the theoretical curve for a gold mirror ( $d = 15$  mm for both).

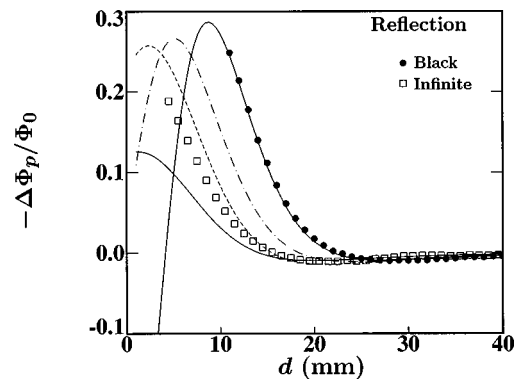


Fig. 5. Sensitivity to scattering  $\Delta\Phi_p/\Phi_0$  in a reflection measurement as a function of the depth  $d$ , with  $\rho_o = \rho_d/2 = 15$  mm, as in Fig. 3. The solid theoretical curves correspond to the data points. The dotted-dashed curve is for an aluminum mirror; the dashed curve is for a gold mirror.

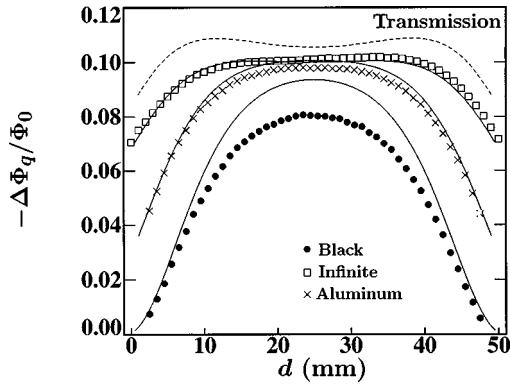


Fig. 6. Sensitivity to absorption  $\Delta\Phi_q/\Phi_0 = qQ$  in a transmission measurement as a function of the depth  $d$ , with  $\rho_o = 15$  mm. The solid curves are the theoretical values; the dashed curve is the theoretical curve for a gold mirror. The thickness of the slab is  $L = 50$  mm.

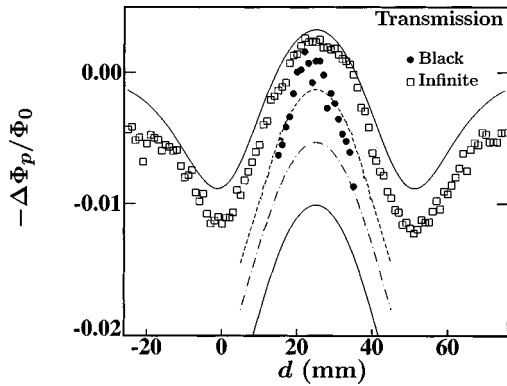


Fig. 7. Sensitivity to scattering  $\Delta\Phi_p/\Phi_0$  in a transmission measurement as a function of the depth  $d$ . The thickness of the slab is  $L = 50$  mm, as in Fig. 6. For the infinite medium (squares),  $\rho_o = 19$  mm; for the semi-infinite medium (dots),  $\rho_o = 15$  mm. Note that the domain of  $d$  for the infinite medium is larger than in Fig. 6. The solid theoretical curves correspond to the data points. The dotted-dashed curve is the theoretical curve for an aluminum mirror; the dashed curve is that for a gold mirror ( $\rho_o = 15$  mm for both).

We also calculated the theoretical curves for an aluminum boundary, which is shown in Figs. 4 and 5; the dotted-dashed curves signify that no experimental results were available, and the dotted curves are for a gold mirror. We observe again that the semi-infinite medium with reflecting boundaries is similar to the infinite medium.

The expression (20) for  $P$  may take on negative values. This happens when the scattering of a photon density wave from the object is effectively backward. Such a negative sensitivity means that the detected signal will increase when the object scatters more strongly. For absorbing objects a change of sign is not possible. For Fig. 4 we observe this effect when  $\rho_o$  is large enough. This implies a faster decrease in  $P$  than that which we observed for  $Q$ . In the geometry of Fig. 5, the sensitivity to scattering  $P$  becomes negative either when  $d$  is large or when  $d$  is small and the boundary is absorbing. In the latter case the photon density wave will travel from the source into the medium and turn back to the object, which

is close to the boundary. There it will reflect effectively backward and propagate to the detector, again avoiding the absorbing boundary. This effectively backward reflection implies a negative sensitivity  $P$ .

To give a full comparison between infinite systems and finite systems with different kinds of boundaries, it is not enough to consider only reflection measurements. As we discussed in Subsection 3.B, for a finite medium all measurements are either like reflection measurements or like transmission measurements. The geometry that we chose for transmission experiments is one where the source and the detector are opposite to each other (head on), as in Fig. 1(b). The thickness of the slab is  $L = 50$  mm. The object is scanned along a line parallel to the source-detector line, at a distance  $\rho_o$ . The depth of the object,  $d$ , is again varied. Results are shown in Figs. 6 and 7 for the absorbing and the scattering object, respectively. We have also theoretically investigated a geometry that is finite in two directions instead of one and found no qualitative difference from the slab.

As is shown in relation (56), the sensitivity in a transmission experiment when the object is not close to a boundary is the same as those for an infinite medium and for a medium with mirrors. The amount of reflection is not very important in this case, as can be observed in Fig. 6. When the object is closer to the boundary, one can again observe differences between good and not-so-good mirrors.

The results shown in Fig. 7 are noisy because of the smallness of  $\Delta\Phi_p/\Phi_0$ . A systematic shift can be observed between the data points of the absorbing medium and the theory. Again, this is due either to a drift in the detector or to a small error in determining the position of the object, which results in larger errors after the subtraction of two measurements. Qualitatively, there is only a slight difference between the different boundaries in this case.

### E. Absorbing Boundaries

Using the experimental results, we could already qualitatively compare the absorbing boundary with the infinite medium. Here we will give some quantitative results to compare the infinite medium with media having absorbing boundaries. To find simple expressions in the case of absorbing boundaries, we will take  $\xi = \xi_{in} + \xi_{ext}$  to be small. This results in approximate expressions that can be used for qualitative discussions. Since the model point source is very close to the boundary, we can take the terms in Eq. (53) pairwise together:

$$G_\infty(\mathbf{r}, \mathbf{r}_s) - G_\infty(\mathbf{r}, \mathbf{r}_s - 2\xi\hat{\mathbf{z}}) \approx 2\xi\hat{\mathbf{z}} \cdot \nabla_{\mathbf{r}_s} G_\infty(\mathbf{r}_d, \mathbf{r}_s - \xi\hat{\mathbf{z}}). \quad (58)$$

We note that the argument  $\mathbf{r}_s - \xi\hat{\mathbf{z}} \equiv \tilde{\mathbf{r}}_s$  is a point at the (extrapolated) boundary. Using relation (58), we can write the following for the total Green function for the slab:

$$G_L(\mathbf{r}, \mathbf{r}_s) = 2\xi\hat{\mathbf{z}} \cdot \nabla_{\tilde{\mathbf{r}}_s} \sum_m G_\infty(\mathbf{r}, \tilde{\mathbf{r}}_s + 2mL\hat{\mathbf{z}}). \quad (59)$$

Since the Green function for the infinite medium depends only on the difference between the two points  $\mathbf{r}$  and  $\mathbf{r}'$ ,

i.e.,  $G_\infty(\mathbf{r}, \mathbf{r}') = G_\infty(\mathbf{r} - \mathbf{r}')$ , we can write the Green function for light going to the detector at position  $\mathbf{r}_d$  as

$$G_L(\mathbf{r}_d, \mathbf{r}) = \pm 2\xi\hat{\mathbf{z}} \cdot \nabla_{\tilde{\mathbf{r}}_d} \sum_m G_\infty(\tilde{\mathbf{r}}_d + 2mL\hat{\mathbf{z}}, \mathbf{r}). \quad (60)$$

Here  $\tilde{\mathbf{r}}_d = \mathbf{r}_d \mp \xi\hat{\mathbf{z}}$  is also a point at the (extrapolated) boundary. The upper signs belong to a reflection measurement, where the detected light propagates in the negative  $z$  direction. The lower signs correspond to a transmission measurement. There can, however, be no doubt about which sign to take, since the Green function is always positive.

For calculating  $G_L(\mathbf{r}_d, \mathbf{r}_s)$ , we can use Eq. (59) and evaluate it at  $\mathbf{r}_d = \tilde{\mathbf{r}}_d \pm \xi\hat{\mathbf{z}}$ . We again use the derivative with respect to  $\tilde{\mathbf{r}}_d$  to find that  $G_L(\mathbf{r}_d, \mathbf{r}_s) = \pm \xi\hat{\mathbf{z}} \cdot \nabla_{\tilde{\mathbf{r}}_d} G_L(\tilde{\mathbf{r}}_d, \mathbf{r}_s)$ . The photon density can now be easily found. When only one absorbing object is present with strength  $q$ , we find that

$$\begin{aligned} \Phi_L(\mathbf{r}_d) &= \frac{S_\omega}{D} \left[ G_L(\mathbf{r}_d, \mathbf{r}_s) + \frac{4\pi q}{\kappa_0} G_L(\mathbf{r}_d, \mathbf{r}_o) G_L(\mathbf{r}_o, \mathbf{r}_s) \right] \\ &= \pm 2\xi^2 \frac{S_\omega}{D} (\hat{\mathbf{z}} \cdot \nabla_{\tilde{\mathbf{r}}_s})(\hat{\mathbf{z}} \cdot \nabla_{\tilde{\mathbf{r}}_d}) \\ &\quad \times \sum_m \left[ G_\infty(\tilde{\mathbf{r}}_d, \tilde{\mathbf{r}}_s + 2mL\hat{\mathbf{z}}) + 2 \frac{4\pi q}{\kappa_0} \right. \\ &\quad \times \sum_{m'} G_\infty(\tilde{\mathbf{r}}_d + 2m'L\hat{\mathbf{z}}, \mathbf{r}_o) \\ &\quad \left. \times G_\infty(\mathbf{r}_o, \tilde{\mathbf{r}}_s + 2mL\hat{\mathbf{z}}) \right]. \quad (61) \end{aligned}$$

In general, the sums over  $m$  and  $m'$  will have only a few terms that are important, which is due to the exponential decay of  $G_\infty$ .

Let us first consider the semi-infinite medium. Since  $L \rightarrow \infty$ , we have only to take  $m = m' = 0$  in the sums. Furthermore, only measurements in reflection are possible. We find from Eq. (61) that

$$\begin{aligned} \Phi_s(\mathbf{r}_d) &= \frac{2\xi^2 S_\omega}{D} (\hat{\mathbf{z}} \cdot \nabla_{\tilde{\mathbf{r}}_s})(\hat{\mathbf{z}} \cdot \nabla_{\tilde{\mathbf{r}}_d}) \left[ G_\infty(\tilde{\mathbf{r}}_d, \tilde{\mathbf{r}}_s) \right. \\ &\quad \left. + \frac{8\pi q}{\kappa_0} G_\infty(\tilde{\mathbf{r}}_d, \mathbf{r}_o) G_\infty(\mathbf{r}_o, \tilde{\mathbf{r}}_s) \right]. \quad (62) \end{aligned}$$

We can compare this with the equation that we would have found in the infinite medium:

$$\Phi_\infty(\mathbf{r}_d) = \frac{S_\omega}{D} \left[ G_\infty(\mathbf{r}_d, \mathbf{r}_s) + \frac{4\pi q}{\kappa_0} G_\infty(\mathbf{r}_d; \mathbf{r}_o) G_\infty(\mathbf{r}_o; \mathbf{r}_s) \right]. \quad (63)$$

So, basically, the photon density at the detector for the semi-infinite medium is given by that for the infinite medium, differentiated to both source and detector position. Furthermore, we see that an extra factor of 2 appeared in front of  $q$ . This enhancement is similar to that of relation (55). The sensitivity to absorption  $Q = (\Phi - \Phi_0)/q\Phi_0$  can be found rather easily from the expressions above.

As an example let us consider the case where source, object, and detector are all in the same plane (see Fig. 1). Only the depth  $d$  of the object into the medium and the lateral distances  $\rho_d$  and  $\rho_0$  are of importance. Define  $d_s = z_o - z_s$  and  $d_d = z_o - z_d$ . Of course,  $d_d$  and  $d_s$  have the same value  $d$ , but the functional dependence of  $\Phi$  on both differs. Hence we have to consider them separately when taking derivatives. The two differential operators become

$$(\hat{\mathbf{z}} \cdot \nabla_{\tilde{\mathbf{r}}_{s,d}}) \rightarrow -\frac{\partial}{\partial d_{s,d}}. \quad (64)$$

Three distances are needed:  $r_1$  from source to object,  $r_2$  from object to detector, and  $r_{12}$  from source to detector. They are given by

$$\begin{aligned} r_1 &= \sqrt{\rho_o^2 + d_s^2}, & r_2 &= \sqrt{(\rho_o - \rho_d)^2 + d_d^2}, \\ r_{12} &= \sqrt{\rho_d^2 + (d_d - d_s)^2}. \end{aligned} \quad (65)$$

We calculate the photon density  $\Phi_\infty$  for the infinite geometry and  $\Phi_s$  for the semi-infinite geometry, both at the detector position  $\mathbf{r}_d$ . The results are

$$\Phi_{0,\infty} = \frac{S_\omega}{4\pi D} \frac{1}{r_{12}} \exp(-\kappa r_{12}), \quad (66a)$$

$$\Delta\Phi_\infty = \frac{S_\omega}{4\pi D} \left\{ \frac{q}{\kappa_0 r_1 r_2} \exp[-\kappa(r_1 + r_2)] \right\}, \quad (66b)$$

$$\Phi_{0,s} = \frac{S_\omega}{4\pi D} 2\xi^2 \frac{1 + \kappa r_{12}}{r_{12}^3} \exp(-\kappa r_{12}), \quad (66c)$$

$$\begin{aligned} \Delta\Phi_s &= \frac{S_\omega}{4\pi D} \left\{ 4q\xi^2 d^2 \frac{(1 + \kappa r_1)(1 + \kappa r_2)}{\kappa_0 r_1^3 r_2^3} \right. \\ &\quad \left. \times \exp[-\kappa(r_1 + r_2)] \right\}. \end{aligned} \quad (66d)$$

From these results we calculate the sensitivities

$$Q_\infty = \frac{r_{12}}{\kappa r_1 r_2} \exp[-\kappa_0(r_1 + r_2 - r_{12})], \quad (67a)$$

$$Q_s = 2 \frac{(1 + \kappa r_1)(1 + \kappa r_2)}{1 + \kappa r_{12}} \frac{d^2 r_{12}^2}{r_1^2 r_2^2} Q_\infty. \quad (67b)$$

We note that these no longer depend on the value of  $\xi$ . The expressions for the sensitivity for scattering can be calculated readily, but they are rather lengthy and will not be presented here.

In many practical cases the ratio  $dr_{12}/r_1 r_2$  will be of the order of 1. Only when the source-detector distance remains fixed and the objects are far from both does this ratio decrease. But then the influence of the object on the measurement is negligible, as a result of the exponential decay of  $Q$ . Hence, in practice,  $Q_s/Q_\infty$  is of the same order as  $1 + \kappa r_{12}$  (which means of the order of 1 when  $\kappa r_{12} \ll 1$  and of the order of  $\kappa r_{12}$  when  $\kappa r_{12} \gg 1$ ). The black boundary can therefore increase sensitivity. A price has to be paid, however. The total intensity detected in the semi-infinite system will be largely decreased with respect to the infinite medium. This can be seen from the ratio

$$\frac{\Phi_{0,\infty}}{\Phi_{0,s}} = 2 \left( \frac{\xi}{r_{12}} \right)^2 (1 + \kappa r_{12}) \quad (\text{in reflection}), \quad (68)$$

which is always small ( $\xi \approx \mu_s^{-1}$ ). (We always assume source–detector distances to be larger than a few scattering lengths.) The decrease in intensity that is due to the finiteness of the medium is due mainly to a loss of intensity at the boundary close to the source and at the boundary close to the detector.

For the quantitative discussion in the slab geometry, we consider only the situation where source, detector, and object are on the same line ( $\rho_o = \rho_d = 0$ ). Furthermore, we assume that the object is not too close to the boundary. Then the result [taking only the most important terms in the sum of Eq. (61)] is

$$Q_\infty = \frac{L}{\kappa_0 r_1 r_2}, \quad (69a)$$

$$Q_{\text{slab}} = \frac{L^2}{r_1 r_2} \frac{(1 + \kappa r_1)(1 + \kappa r_2)}{2 + 2\kappa L + \kappa^2 L^2} Q_\infty, \quad (69b)$$

$$P_\infty = \frac{(1 + \kappa r_1)(1 + \kappa r_2)L}{\kappa_0^3 r_1^2 r_2^2}, \quad (69c)$$

$$P_{\text{slab}} = \frac{(2 + 2\kappa r_1 + \kappa^2 r_1^2)(2 + 2\kappa r_2 + \kappa^2 r_2^2)L^3}{(2 + 2\kappa L + \kappa^2 L^2)\kappa_0^3 r_1^3 r_2^3}. \quad (69d)$$

Note that  $r_1 + r_2 = L$ . From this we find that for large  $\kappa$  there is no difference in the sensitivities between the slab and the infinite system. This is basically due to the fact that for large absorption a boundary has only a local effect. At the position of the object or the detector, the difference between a source at a boundary and a source in an infinite medium is no longer visible, apart from an overall prefactor. The same holds for the boundary at the position of the detector. Therefore the sensitivity is the same in both cases. This is not true in a reflection measurement, where the influence of the boundary on the propagation from source to detector is no longer local but can be felt everywhere between source and detector. Therefore, for large  $\kappa$  and in reflection, the sensitivities for an infinite medium and for a bounded medium will be different. For small  $\kappa$  the sensitivity  $Q_{\text{slab}}$  will be a factor of  $L^2/2r_1 r_2 > 2$  larger than  $Q_\infty$ , and  $P_{\text{slab}}$  will be a factor of  $2L^2/r_1 r_2 > 8$  larger than  $P_\infty$ . From the expressions we also see that the sensitivities can be large for small  $r_1$  or  $r_2$ , increasing the sensitivity when the object is close to source or detector, even more so when the boundaries are absorbing. The expressions (69) are, however, are no longer correct close to the boundary.

Again, we note that the enhancement is relatively small compared with the loss in detected signal. The ratio between the detected signals in this geometry is given by

$$\frac{\Phi_{\text{slab}}}{\Phi_\infty} = \left( \frac{\xi}{L} \right)^2 (2 + 2\kappa L + \kappa^2 L^2) \quad (\text{in transmission}). \quad (70)$$

As was the case in the semi-infinite geometry, this ratio is small, mainly because of the  $\xi^2$  term, which is a result of the boundary. Hence, again, a large price has to be paid to increase sensitivity.

In comparing the infinite medium with the semi-infinite medium with absorbing boundaries, we comment on some other features. Consider again Fig. 3. All curves show a maximum at some depth  $d$  and a decrease in the sensitivity for larger depths. The difference between the different boundaries seems to be only in the position of this maximum, giving the position of the maximum sensitivity. The sensitivities for an infinite medium are centered on the line between source and detector. One can say that the photon density wave propagates along this line, although, of course, single light paths can be much more complex. For absorbing boundaries the Green functions and therefore the sensitivities (almost) vanish at the boundaries. This implies that when the line between source and detector lies close to a boundary, the centerline of the sensitivity—the line where for different  $\rho_o$  the maximum value of  $Q$  can be found—will curve away from this boundary. Consequently, the propagation direction will be curved (see Fig. 8). The maximum shown in Fig. 3 lies away from the boundary, at larger depths than that of the infinite medium (or the medium with reflecting boundaries). This means that the semi-infinite medium is not really more sensitive to absorbing objects; rather, the spatial location of this sensitivity is changed.

As a next point we note that the strength  $p$  of the scattering object [calculated by using the first of Eqs. (23)] is approximately four times smaller than the strength  $q$  of the absorbing object that we used. Furthermore, the scattering object is large, and therefore it has some parts in regions with low sensitivity for scattering. Nonetheless, the measured effects are almost as big as those of absorbing objects, at least in reflection measurements. Apparently, the sensitivity for scattering  $P$  is generally larger than the sensitivity for absorption  $Q$ . The difference of approximately a factor of 5 appears mainly close to the boundary, and for absorbing boundaries almost everywhere. The latter is due to two reasons. First, scattering objects have an influence that scales with the gradient of the Green function rather than with the Green

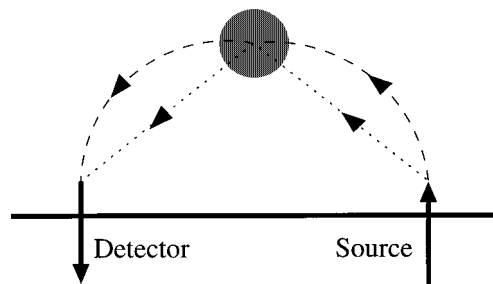


Fig. 8. Schematic view of the propagation of the photon density in a reflection measurement, as shown schematically in Fig. 1. The arrows show the average direction of the photon density flow. The two solid arrows show the propagation of light in and just outside the source and detector fiber. The dotted arrows are for an infinite medium, where propagation is direct. The dashed arrows are for a semi-infinite medium with absorbing boundaries, where the propagation avoids the boundary.

function itself. Since the decrease of  $G$  is larger for an absorbing boundary, the sensitivity will increase. Second, consider the position at  $\rho_o = 15$  mm and  $d = 10$  mm, which can be found in both Figs. 2 and 3. For the infinite medium an extra term  $\cos \theta$  appears in the sensitivity, where  $\theta$  is the angle between the source-object and object-detector lines. This term enters as a result of the inner product. In the semi-infinite medium, however, the angle  $\theta$ , which is the angle between the two gradients of the Green function, will be smaller. This reflects a photon density wave that does not propagate straight from source to object. As discussed above and shown schematically in Fig. 8, the propagation will rather be curved on account of the absorbing boundary. Upon arriving at the object, it will propagate more parallel to the boundary than in the infinite medium. Also, the propagation from object to detector will be such that its direction at the object is almost parallel to the boundary. The effective  $\cos \theta$  will therefore be larger than in the infinite medium.

The difference between the sensitivities for absorption and scattering implies that  $|\Delta\Phi/\Phi_0|$  is larger for an object with a given  $\Delta D/D$  than for an object with the same  $\Delta\mu_a/\mu_a$ . In practice, however, the variation in absorption can be 1 order of magnitude larger than the variation in scattering. Therefore measurements will, in general, be more sensitive to absorption than to scattering.

#### 4. CONCLUSIONS

We have studied the influence of different boundaries on the detection of objects. To do this, we started with a derivation of the expressions that give the values of the photon density—which is proportional to measured data—when the optical parameters are not constant but rather vary in space. We have shown a clear distinction between geometrical factors, given by the sensitivities  $Q$  and  $P$ , and the strengths  $q$  and  $p$  of (small) objects. These can be calculated independently. We have shown how to calculate the strengths even when the scattering or the absorption in the object is not small and have improved the expressions from the literature for a completely black spherical object.

The experiments that we performed are done with a cylindrical object, whereas the theoretical value of  $q$  was derived only for a spherical object. From this we note two things. First, experimentally it is nearly impossible to see the difference between different shapes of objects, in our case a sphere and a cylinder. As mentioned above, this means that, for small objects, only the value  $q$  (or  $p$ ) can be measured and that nearly nothing about the precise shape can be found. Second, even though we did not calculate the exact value of  $q$  for a cylindrical object, we are able to give a rather good estimate by using the theory for a sphere.

Next, we have compared the different boundaries. For a boundary of a good mirror, such as gold, the sensitivity is merely a constant times the sensitivity of an infinite medium. This constant is nearly 2 for a measurement in reflection and approximately 1 for a measurement in transmission. For a medium with absorbing boundaries, the sensitivity in reflection can become rather large, when

the decay constant  $\kappa$  is large, compared with the inverse source-detector distance. For moderate  $\kappa$ , however, the difference with an infinite medium lies mainly in the spatial position of the sensitivity rather than in the values themselves. Close to absorbing boundaries the sensitivity vanishes. For a system bounded by a not-so-good mirror, such as the aluminum mirror that we used in the experiments, the sensitivity is between that of an infinite medium and that of a medium with absorbing boundaries.

Considering the effects of sensitivity to the object and total intensity detected, we see that there is a trade-off between the two. Since the effect of loss of intensity when black boundaries are used is much larger than the gain in sensitivity, we argue that for detecting objects an infinite system, or one with good mirrors, is better than a finite one, or one with not-so-good mirrors. Furthermore, the infinite medium has another advantage: formulas, such as those for the photon density and the sensitivities, will be simpler. This simplifies the reconstruction of inhomogeneities inside the turbid medium. Since, in practice, an infinite medium is difficult to achieve in the circumstances needed for medical imaging, a finite system with a rather good reflecting boundary resembles the infinite medium enough to be useful for both forward calculations and reconstruction techniques.

#### ACKNOWLEDGMENTS

We thank J. H. Hoogenraad, C. W. J. Beenakker, M. B. van der Mark, and J. B. M. Melissen for inspiring discussions. This work was supported by the Nederlandse organisatie voor Wetenschappelijk Onderzoek.

#### REFERENCES

1. P. N. den Outer, Th. M. Nieuwenhuizen, and A. Lagendijk, "Location of objects in multiple-scattering media," *J. Opt. Soc. Am. A* **10**, 1209–1218 (1993).
2. X. D. Zhu, S. Wei, S. C. Feng, and B. Chance, "Analysis of a diffuse-photon-density wave in multiple-scattering media in the presence of a small spherical object," *J. Opt. Soc. Am. A* **13**, 494–499 (1996).
3. R. C. Haskell, L. O. Svaasand, T. Tsay, T. Feng, M. S. McAdams, and B. J. Tromberg, "Boundary conditions for the diffusion equation in radiative transfer," *J. Opt. Soc. Am. A* **11**, 2727–2741 (1994).
4. A. Ishimaru, *Wave Propagation and Scattering in Random Media* (Academic, New York, 1978).
5. W. M. Star, "Diffusion theory of light transport," in *Optical-Thermal Response of Laser-Irradiated Tissue*, A. J. Welch and M. J. C. van Gemert, eds. (Plenum, New York, 1995), pp. 131–206.
6. D. A. Boas, M. A. O'Leary, B. Chance, and A. G. Yodh, "Scattering of diffusive photon density waves by spherical inhomogeneities within turbid media: analytic solution and applications," *Proc. Natl. Acad. Sci. USA* **91**, 4887–4891 (1994).
7. A. Ya Polishchuk, S. Gutman, M. Lax, and R. R. Alfano, "Photon-density modes beyond the diffusion approximation: scalar wave-diffusion equation," *J. Opt. Soc. Am. A* **14**, 230–234 (1997).
8. K. Furutsu and Y. Yamada, "Diffusion approximation for a dissipative random medium and the applications," *Phys. Rev. E* **50**, 3634–3640 (1994).
9. M. Bassani, F. Martelli, G. Zaccanti, and D. Contini, "Independence of the diffusion coefficient from absorption: experimental and numerical evidence," *Opt. Lett.* **22**, 853–855 (1997).

10. K. M. Case and P. F. Zweifel, *Linear Transport Theory* (Addison-Wesley, Reading, Mass., 1967).
11. R. Freyer, U. Hampel, M. Forejtek, and C. T. Luu, "Detection of local inhomogeneities in scattering media using tomographic reconstruction techniques," in *Proceedings of Photon Propagation in Tissues*, B. Chance, D. T. Delpy, G. J. Müller, and A. Katzir, eds., Proc. SPIE **2626**, 316–327 (1995).
12. M. R. Ostermeyer and S. L. Jacques, "Perturbation theory for diffuse light transport in complex biological tissues," *J. Opt. Soc. Am. A* **14**, 255–261 (1997).
13. S. R. Arridge, M. Schweiger, M. Hiraoka, and D. T. Delpy, "A finite element approach for modeling photon transport in tissue," *Med. Phys.* **20**, 299–309 (1993).
14. H. Jiang, K. D. Paulsen, and U. L. Osterberg, "Optical image reconstruction using DC data: simulations and experiments," *Phys. Med. Biol.* **41**, 1483–1498 (1996).
15. S. B. Colak, D. G. Papaioannou, G. W. 't Hooft, M. B. van der Mark, H. Schomberg, J. C. J. Paasschens, J. B. M. Mellissen, and N. A. A. J. van Asten, "Tomographic image reconstruction from optical projections in light-diffusing media," *Appl. Opt.* **36**, 180–213 (1997).
16. Y. Yao, Y. Wang, Y. Pei, W. Zhu, and R. L. Barbour, "Frequency-domain optical imaging of absorption and scattering distributions by a Born iterative method," *J. Opt. Soc. Am. A* **14**, 325–342 (1997).
17. W. Zhu, Y. Wang, Y. Yao, J. Chang, H. L. Graber, and R. L. Barbour, "Iterative total least-squares image-reconstruction algorithm for optical tomography by the conjugate-gradient method," *J. Opt. Soc. Am. A* **14**, 799–807 (1997).
18. S. Feng, F. Zeng, and B. Chance, "Monte Carlo simulations of photon migration path distributions in multiple scattering media," in *Photon Migration and Imaging in Random Media and Tissues*, B. Chance and R. R. Alfano, eds., Proc. SPIE **1888**, 78–89 (1993).
19. J. C. Schotland, J. C. Haselgrove, and J. S. Leigh, "Photon hitting density," *Appl. Opt.* **32**, 448–453 (1993).
20. S. Feng, F. Zeng, and B. Chance, "Photon migration in the presence of a single defect: a perturbation analysis," *Appl. Opt.* **34**, 3826–3837 (1995).
21. Th. M. Nieuwenhuizen and M. C. W. van Rossum, "Role of a single scatterer in a multiple scattering medium," *Phys. Lett. A* **177**, 102–106 (1993).
22. J. X. Zhu, D. J. Pine, and D. A. Weitz, "Internal reflection of diffusive light in random media," *Phys. Rev. A* **44**, 3948–3959 (1991).
23. R. Aronson, "Extrapolation distance for diffusion of light," in *Photon Migration and Imaging in Random Media and Tissues*, B. Chance and R. R. Alfano, eds., Proc. SPIE **1888**, 297–305 (1993).
24. Th. M. Nieuwenhuizen and J. M. Luck, "Skin layer of diffusive media," *Phys. Rev. E* **48**, 569–588 (1993).
25. A. Yodh and B. Chance, "Spectroscopy and imaging with diffusing light," *Phys. Today* **48** (March), 34–40 (1995).
26. S. Fantini, M. A. Franceschini-Fantini, J. S. Maier, S. A. Walker, B. Barbieri, and E. Gratton, "Frequency-domain multichannel optical detector for noninvasive tissue spectroscopy and oximetry," *Opt. Eng. (Bellingham)* **34**, 32–42 (1995).
27. D. J. Durian, "Influence of boundary reflection and refraction on diffusive photon transport," *Phys. Rev. E* **50**, 857–866 (1994).
28. C. P. Gonatas, M. Miwa, M. Ishii, J. Schotland, B. Chance, and J. S. Leigh, "Effects due to geometry and boundary conditions in multiple light scattering," *Phys. Rev. E* **48**, 2212–2216 (1993).
29. S. Chandrasekhar, *Radiative Transfer* (Dover, New York, 1960).
30. S. R. Arridge, M. Cope, and D. T. Delpy, "The theoretical basis for the determination of optical pathlengths in tissue: temporal and frequency analysis," *Phys. Med. Biol.* **37**, 1531–1560 (1992).
31. S. Fantini, M. A. Franceschini, and E. Gratton, "Semi-infinite-geometry boundary problem for light migration in highly scattering media: a frequency-domain study in the diffusion approximation," *J. Opt. Soc. Am. B* **11**, 2128–2138 (1994).
32. M. S. Patterson, B. Chance, and B. C. Wilson, "Time resolved reflectance and transmittance for the non-invasive measurement of tissue optical properties," *Appl. Opt.* **28**, 2331–2336 (1989).
33. M. N. Barber and B. W. Ninham, *Random and Restricted Walks* (Gordon and Breach, New York, 1970).